J|A|C|S
ARTICLES
Published on Web 03/13/2004

$Mn_{14}Al_{56+x}Ge_{3-x}$ ($x = 0-0.6$): A New Intermetallic Phase Containing Unprecedented "Half-Broken" Mackay Icosahedra as Building Units

Li-Ming Wu and Dong-Kyun Seo*

Contribution from the Department of Chemistry and Biochemistry, Arizona State University, Tempe, Arizona 85287-1604

Received October 21, 2003; E-mail: dseo@asu.edu

Abstract: The new $Mn_{14}Al_{56+x}Ge_{3-x}$ ($x = 0-0.6$) compounds of a new structure type have been synthesized and characterized by physical property measurements and electronic structure calculations. In contrast to their well-known silicon analogues, their unique structure ($P\bar{3}$) exhibits unprecedented partially destroyed Mackay icosahedra that retain the icosahedral symmetry only in half of the individual polyhedra. The electronic band-structure analysis indicates that the chemical bonding in the structure is still optimized despite the destruction of the Mackay icosahedra and that a further valence electron concentration (VEC) optimization is achieved by the partial occupation of aluminum on a germanium site. The electronic band-structure calculation results were in agreement with the poor metallicity observed for the samples. While the $Mn_{14}Al_{56}Ge_3$ is metallic, the resistivity of $Mn_{14}Al_{56.6}Ge_{2.4}$ shows a minimum around 20 K and a maximum around 100 K. Both of the samples are Pauli-paramagnetic with an additional small Curie component.

Introduction

Since the discovery of a quasicrystalline structure in the Mn−Al system,[1,2] there have been renewed interests in crystalline materials whose structures exhibit icosahedral coordination of atoms by their nearest neighboring atoms, in particular tetrahedrally close-packed compounds including Frank−Kasper phases.[3−5] More specifically related are the so-called quasicrystal approximants, whose network structures contain high-symmetry polyhedra that can be used as possible models for components of quasicrystalline structures.[6−10] Structural principles illustrated by the approximants, together with their general physicochemical features, have been indispensable for the studies of quasicrystals because of the fact that the apparent absence of translational symmetries in the quasicrystalline phases creates complex structural problems to solve and hence hinders a more direct understanding of their structure−property relationships. One well-known example is the icosahedral quasicrystal *i*-Mn−Al−Si (a close composition is $Mn_{20}Al_{74}Si_6$) and its approximant α-Mn−Al−Si (a close composition is $Mn_{17.4}Al_{72.5}Si_{10.1}$) from their very closely related electron diffraction patterns as well as the common existence of Mackay icosahedra in their structures.[11,12] Further similarities have been noted in their electronic structures, in that both their complicated chemical structures provide a distinct minimum or a pseudogap in the total electronic density of states (DOSs) at the Fermi energy,[13] indicative of Hume−Rothery "electron compounds".[14] Such electronic contribution to the structure formation also finds its relevance in the studies of polar intermetallics and Zintl compounds for which the valence electron concentration (VEC) has long been considered vital in structure selection.[15,16] Recent advances in this research area have revealed, however, that the atomic sizes and electrostatic energies also need to be considered in many cases for a complete understanding of structure selection of those compounds,[17−21] which certainly shares its essence with the previously recognized size/electronegativity effect in the structures of Laves intermetallic phases[22,23] and more distantly with

(1) Shechtman, D.; Blech, I.; Gratias, D.; Cahn, J. W. *Phys. Rev. Lett.* **1984**, *53*, 1951.
(2) Quasicrystals, or more precisely "quasiperiodic crystals", are materials with perfect long-range order, but with no three-dimensional translational periodicity. The former is manifested in the occurrence of sharp diffraction spots and the latter in the presence of a noncrystallographic rotational symmetry. Icosahedral or dodecahedral units are presumed to be the building blocks of the quasicrystals.
(3) Suck, J.-B. In *Quasicrystals: An Introduction to Structure, Physical Properties, and Applications*; Suck, J.-B., Schreiber, M., Häussler, P., Eds.; Springer: Berlin, 2002.
(4) Frank, F. C.; Kasper, J. S. *Acta Crystallogr.* **1959**, *12*, 483.
(5) Shoemaker, D. P.; Shoemaker, C. B. *Mater. Sci. Forum* **1987**, *22−24*, 67.
(6) Janot, C. *Quasicrystals: A Primer*, 2nd ed.; Oxford University Press: Oxford, U.K., 1994.
(7) Goldman, A. I.; Kelton, R. F. *Rev. Mod. Phys.* **1993**, *65*, 213.
(8) Lee, C. S.; Miller, G. J. *Angew. Chem., Int. Ed.* **2001**, *40*, 4740.
(9) Lee, C. S.; Miller, G. J. *Inorg. Chem.* **2001**, *40*, 338.
(10) Lee, C. S.; Miller, G. J. *J. Am. Chem. Soc.* **2000**, *122*, 4937.
(11) It is emphasized that a Mackay icosahedron is *not* just an icosahedron but one enclosed in the dual M_{42} polyhedron as an outer shell.
(12) (a) Elser, V.; Henley, C. L. *Phys. Rev. Lett.* **1985**, *55*, 2883. (b) Hansen, V.; Gjonnes, J. *Acta Crystallogr. A* **1996**, *52*, 125.
(13) Fujiwara, T. *Curr. Opin. Solid State Mater. Sci.* **1999**, *4*, 295.
(14) De Laissardiere, G. T.; Manh, D. N.; Magaud, L.; Julien, J. P.; Cyrot-Lackmann, F.; Mayou, D. *Phys. Rev. B* **1995**, *52*, 7920.
(15) Nesper, R. *Angew. Chem., Int. Ed. Engl.* **1991**, *30*, 789.
(16) Miller, G. J. In *Chemistry, Structure, and Bonding of Zintl Phases and Ions*; Kauzlarich, S. M., Ed.; VCH: New York, 1996.
(17) Zurcher, F.; Nesper, R. *Angew. Chem., Int. Ed.* **1998**, *37*, 3314.
(18) Seo, D.-K.; Corbett, J. D. *J. Am. Chem. Soc.* **2000**, *122*, 9621.
(19) Seo, D.-K.; Corbett, J. D. *J. Am. Chem. Soc.* **2001**, *123*, 4512.
(20) Seo, D.-K.; Corbett, J. D. *Science* **2001**, *291*, 841.
(21) Seo, D.-K.; Corbett, J. D. *J. Am. Chem. Soc.* **2002**, *124*, 415.
(22) (a) Häussermann, U.; Amerioun, S.; Eriksson, L.; Lee, C.-S.; Miller, G. J. *J. Am. Chem. Soc.* **2002**, *124*, 4371. (b) Amerioun, S.; Simak, S. I.; Häussermann, U. *Inorg. Chem.* **2003**, *42*, 1467.
(23) O'Keeffe, M.; Hyde, B. G. *Crystal Structures: I. Patterns and Symmetry*; Mineralogical Society of America: Washington, DC, 1996.

10.1021/ja039154f CCC: $27.50

Hume-Rothery's size rule in alloy formations.[24] Whether the same holds or not specifically for the quasicrystals and the approximants could be an interesting question in regard to the fundamental understanding of structure-building principles as well as possible material designs via structural modifications of those phases. While we were recently exploring such possibilities in the Mn−Al system, we encountered a new thermodynamically stable crystalline phase, $Mn_{14}Al_{56+x}Ge_{3-x}$ ($x = 0-0.6$), whose atomic ratios (~19:77:4, i.e., $Mn_{19}Al_{77}Ge_4$) quite resemble those of α-Mn−Al−Si, yet with a larger element, Ge.[25] We report here the remarkable structure of the $Mn_{14}Al_{56+x}Ge_{3-x}$ phase, which exhibits unprecedented "half-broken" Mackay icosahedra, and we present their electronic and physical properties.

Experimental Section

Synthesis. The single crystals of the title phase were first obtained by slowly cooling from 1273 K the melt of Mn, Ge, and Al elements at 1:4:20 molar ratio in a graphite crucible contained in an evacuated and flame-sealed fused silica tube. Well-shaped silvery crystals were found on the surface of the gray solid matrix after the reactions. Subsequent single-crystal X-ray diffraction studies on several crystals established the structure and the overall composition $Mn_{14}Al_{56+x}Ge_{3-x}$ with subtle differences among the crystals in Ge and Al contents due to a Ge site that was partially substituted by Al. Afterward, reaction mixtures were loaded accordingly with two different compositions, $Mn_{14}Al_{56}Ge_3$ and $Mn_{14}Al_{56.6}Ge_{2.4}$, in graphite crucibles that were placed in evacuated and flame-sealed fused silica tubes. The reaction containers were heated to 1273 K for 3 h and then quenched to room temperature. The samples were then annealed at 873 K for 2 weeks and cooled radiatively to room temperature. All the products were silvery and brittle and were stable in air for more than several months. The powder X-ray diffraction patterns showed that the products were single phases. Crystals were collected again from the reaction products, and the stoichiometries obtained from their single-crystal X-ray diffraction data [$Mn_{14}Al_{56}Ge_3$ and $Mn_{14}Al_{56.61(1)}Ge_{2.39(1)}$, respectively] were in agreement with the loaded compositions. Crystals with an intermediate composition [for example, $Mn_{14}Al_{56.32(1)}Ge_{2.68(1)}$] also were found in the original slowly cooled reaction product, which strongly supports the possibility of a continuous phase width from $x = 0$ to 0.6. The crystallographic information for $Mn_{14}Al_{56.32(1)}Ge_{2.68(1)}$ can be found in the Supporting Information. It is possible that the actual phase width can even increase for this new phase, and further studies are required for a complete composition range. Energy-dispersive X-ray spectroscopic analysis confirmed the stoichiometries of the reaction products within the instrumental error limit but did not allow us to differentiate the small differences in the exact amounts of Ge in the samples.

Structure Determination: $Mn_{14}Al_{56}Ge_3$. A shiny silvery block-shaped crystal, ~0.06 × 0.04 × 0.03 mm^3, was mounted on a thin glass rod with an epoxy glue. The crystal was transferred to a Bruker-AXS Smart Apex CCD-equipped X-ray diffractometer. The crystal quality was first checked from a rotation photograph. The data collection took place at 25 °C with monochromated Mo Kα radiation. A total of 1818 frames was collected from three sets of 0.3° scans in ω at ϕ settings of 0°, 120°, and 240° with an exposure time of 30 s/frame. The reflection intensities were integrated with the SAINT subprogram in the SMART software package[26] for the hexagonal cell initially indicated from indexing 787 reflections. This process yielded a total of 13 099 reflections, out of which 2165 were independent and 2048 had intensities greater than $2\sigma(I)$. The XPREP subprogram in the SHELXTL software package[27] was used for space group determination, in which systematic absences indicated $P\bar{3}$ and $P3$ as possible space groups. The intensity statistics indicated a centrosymmetric space group ($\langle E^2 - 1\rangle = 0.966$), and the subsequent refinement with $P\bar{3}$ provided a satisfactory result in the later steps. The initial model was obtained from the direct method. Data were initially corrected for absorption by use of the SADABS routine in the SAINT subprogram. The full-matrix least-squares refinement converged at $R(F) = 4.7\%$, w$R2 = 8.7\%$, and GOF = 1.07 for 112 variables and 2165 reflections. The largest residual peak and hole in the ΔF map were 0.873 and −1.182 e Å^{-3}, respectively. The atomic positions were standardized by use of the STRUCTURE TIDY program.[28] Some aspects of the data collection and refinement are listed in Table 1. Table 2 gives the atomic positional and isotropic equivalent displacement parameters. Important interatomic distances and bond angles in the structure are given in the Supporting Information.

Table 1. Selected Data Collection and Refinement Parameters for $Mn_{14}Al_{56+x}Ge_{3-x}$ ($x = 0-0.6$)

	$Mn_{14}Al_{56}Ge_3$
space group, Z	$P\bar{3}$ (no. 147), 1
formula weight	2497.81
lattice parameters (Å)	$a = 11.098(2)$, $b = 11.098(2)$, $c = 10.350(2)$
ρ_{calcd} (g·cm^{-3})	3.757
μ(Mo Kα, cm^{-1})	69.97
$R1$, $wR2$[a]	0.0465, 0.0865
	$Mn_{14}Al_{56.6}Ge_{2.4}$
space group, Z	$P\bar{3}$ (no. 147), 1
formula weight	2469.99
lattice parameters (Å)	$a = 11.103(2)$, $b = 11.103(2)$, $c = 10.354(2)$
ρ_{calcd} (g·cm^{-3})	3.710
μ(Mo Kα,cm^{-1})	65.93
$R1$, $wR2$[b]	0.0454, 0.0679

[a] $R1 = \sum||F_o| - |F_c||/\sum|F_o|$, $wR2 = [\sum w(|F_o|^2 - |F_c|^2)^2/\sum w(F_o^2)]^{1/2}$, where $w = 1/[\sigma^2(|F_o|^2) + 9.8415P]$and $P = (F_o^2 + 2F_c^2)/3$. [b] $R1 = \sum||F_o| - |F_c||/\sum|F_o|$, $wR2 = [\sum w(|F_o|^2 - |F_c|^2)^2/\sum w(F_o^2)]^{1/2}$, where $w = 1/[\sigma^2(|F_o|^2) + (0.0208P)^2]$ and $P = (F_o^2 + 2F_c^2)/3$.

$Mn_{14}Al_{56.61(1)}Ge_{2.39(1)}$. A silvery block-shaped crystal, ~0.05 × 0.04 × 0.03 mm^3, was used for data collection, data correction, and structure determination, which were carried out in the same way as for the $Mn_{14}Al_{56}Ge_3$ product. From a total of 13 161 reflections, 2170 were independent and 1935 had intensities greater than 2σ(I). The unit cell was determined from 832 reflections, and the $P\bar{3}$ space group was chosen from the observed systematic absences and the intensity statistics ($\langle E^2 - 1\rangle = 0.971$). The refinement converged with $R(F) = 4.5\%$, w$R2 = 6.8\%$, and GOF = 1.08 for 114 variables and 2170 reflections. The largest residual peak and hole in the ΔF map were 0.898 and −0.820 e Å^{-3}, respectively. Tables 1 and 2 show selected crystallographic data, and more structural parameters are given in the Supporting Information. An equally satisfactory structure refinement was achieved on the basis of the assumption of Mn/Ge partial occupancy on the Ge site [Ge(2) in Table 2] in the Mn@Al_9Ge cluster (see below). However, the Ge site was occupied 78% by Mn and 22% by Ge in the final structure, which was unreasonable for the longer bond distances found around the Ge site [$d(Ge-Al)_{min} = 2.74$ Å vs $d(Mn-Al)_{min} = 2.43-2.53$ Å].

Properties. A standard four-probe technique was used to measure the temperature-dependent resistivity for the cold-pressed samples of $Mn_{14}Al_{56}Ge_3$ and $Mn_{14}Al_{56.6}Ge_{2.4}$ with dimensions of 1 × 1 × 3 mm^3 from 1.8 to 300 K, on a Quantum Design superconducting quantum

(24) Hume−Rothery, W. *Electrons, Atoms, Metals, and Alloys*, 3rd ed.; Dover: New York, 1963.
(25) Some quasicrystalline and cubic approximant phases have been observed from the rapidly solidified melts in the Mn−Al−Ge system. Their structures are not known except that they all appear to have icosahedral building units from their electron diffraction patterns. See, for example, (a) Lalla, N. P.; Tiwari, R. S.; Srivastava, O. N. *J. Mater. Res.* **1992**, *7*, 53. (b) Yokoyama, Y.; Inoue, A.; Note, R.; Kaneko, T. *Mater. Trans., JIM* **1998**, *39*, 237.
(26) *SMART*; Bruker AXS, Inc.: Madison, WI, 1996.
(27) *SHELXTL*; Bruker AXS, Inc.: Madison, WI, 1997.
(28) Gelato, L. M.; Parthé, E. *J. Appl. Crystallogr.* **1987**, *20*, 139.

Table 2. Atomic Coordinates ($\times 10^4$ Å) and Isotropic Equivalent Displacement Parameters ($\times 10^3$ Å^2) for $Mn_{14}Al_{56+x}Ge_{3-x}$ (x = 0−0.6)

	Wyck	x	y	z	B_{eq}[a]
		$Mn_{14}Al_{56}Ge_3$			
Mn(1)	2*d*	3333	6667	4454(1)	4(1)
Mn(2)	6*g*	3609(1)	4229(1)	716(1)	5(1)
Mn(3)	6*g*	2579(1)	483(1)	3312(1)	5(1)
Ge(1)	1*a*	0	0	0	7(1)
Ge(2)	2*d*	3333	6667	7205(1)	11(1)
Al(1)	2*c*	0	0	7452(2)	9(1)
Al(2)	6*g*	2622(1)	1308(1)	843(1)	9(1)
Al(3)	6*g*	4929(1)	1144(1)	4364(1)	9(1)
Al(4)	6*g*	1382(1)	4166(1)	4532(1)	11(1)
Al(5)	6*g*	1674(2)	6242(2)	2736(1)	12(1)
Al(6)	6*g*	1920(1)	5132(1)	159(1)	8(1)
Al(7)	6*g*	4477(1)	634(1)	1710(1)	9(1)
Al(8)	6*g*	4074(1)	3050(1)	2690(1)	8(1)
Al(9)	6*g*	1456(1)	3002(1)	1880(1)	9(1)
Al(10)	6*g*	1665(1)	1950(1)	4218(1)	8(1)
		$Mn_{14}Al_{56.6}Ge_{2.4}$			
Mn(1)	2*d*	3333	6667	4442(1)	5(1)
Mn(2)	6*g*	3606(1)	4229(1)	709(1)	6(1)
Mn(3)	6*g*	2578(1)	485(1)	3310(1)	6(1)
Ge(1)	1*a*	0	0	0	8(1)
Ge(2)/Al(12)[b]	2*d*	3333	6667	7197(1)	11(1)
Al(1)	2*c*	0	0	7446(2)	10(1)
Al(2)	6*g*	2622(1)	1309(1)	842(1)	10(1)
Al(3)	6*g*	4929(1)	1153(1)	4373(1)	10(1)
Al(4)	6*g*	1379(1)	4173(1)	4516(1)	12(1)
Al(5)	6*g*	1684(1)	6254(1)	2722(1)	13(1)
Al(6)	6*g*	1921(1)	5132(1)	147(1)	9(1)
Al(7)	6*g*	4485(1)	640(1)	1719(1)	10(1)
Al(8)	6*g*	4068(1)	3050(1)	2690(1)	9(1)
Al(9)	6*g*	1451(1)	2995(1)	1876(1)	11(1)
Al(10)	6*g*	1671(1)	1958(1)	4220(1)	9(1)

[a] B_{eq} is defined as a third of the trace of the orthogonalized $\mathbf{U}_{ij}$ tensor. [b] Ge:Al = 0.694(3):0.306(3)

interference device (SQUID) magnetometer. Magnetic susceptibility measurements for the samples were performed on powder samples at 3 T over the temperature range from 3 to 300 K.

Electronic Structure Calculations. The tight-binding linear muffin-tin orbital (TB-LMTO) band calculations were performed by use of the LmtART 6.20 program package.[29] The atomic sphere approximation (ASA) was employed, and the density functional was calculated by utilizing the Vosko−Wilk−Nussair method for the local density approximation (LDA).[30] A total of 27 *k*-points was used for Brilloun zone integrations.

Results and Discussion

Structural Description. A [001] projection view of the structure of $Mn_{14}Al_{56+x}Ge_{3-x}$ (space group $P\bar{3}$) is shown in Figure 1. A convenient way to describe the structure is first to identify structural building units that are reminiscent of the high-symmetry polyhedra found in the approximants and presumably quasicrystals. A careful examination reveals that such polyhedral structures exist around only one atomic site in the $Mn_{14}Al_{56+x}Ge_{3-x}$ structure, which is one of three inequivalent Mn positions, Mn(1). As shown in Figure 2a, the Mn position is surrounded by a 10-membered Al_9Ge polyhedron as its first shell to form a [Mn@Al_9Ge] cluster [d(Mn−Al) = 2.43−2.54 Å; d(Mn−Ge) = 2.85 Å]. The cluster can be considered as an incomplete variant of an icosahedron; i.e., it is derived by replacing one triangular face at the bottom of the icosahedron

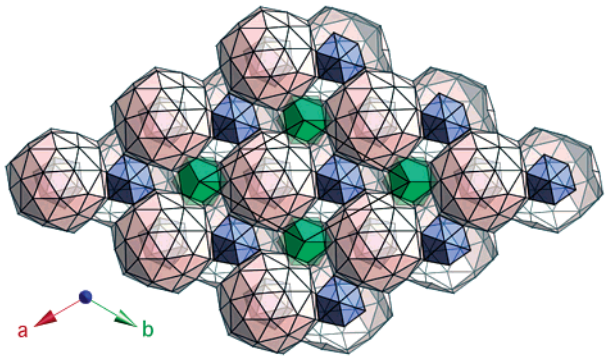

Figure 1. [001] Projection view of the trigonal $Mn_{14}Al_{56+x}Ge_{3-x}$ structure. The blue and green polyhedra represent [Mn@Al_9Ge] and [Ge@Al_8] clusters, respectively. The pale pink polyhedra are "half-broken" Mackay icosahedra and they surround the half-portion of [Mn@Al_9Ge] clusters.

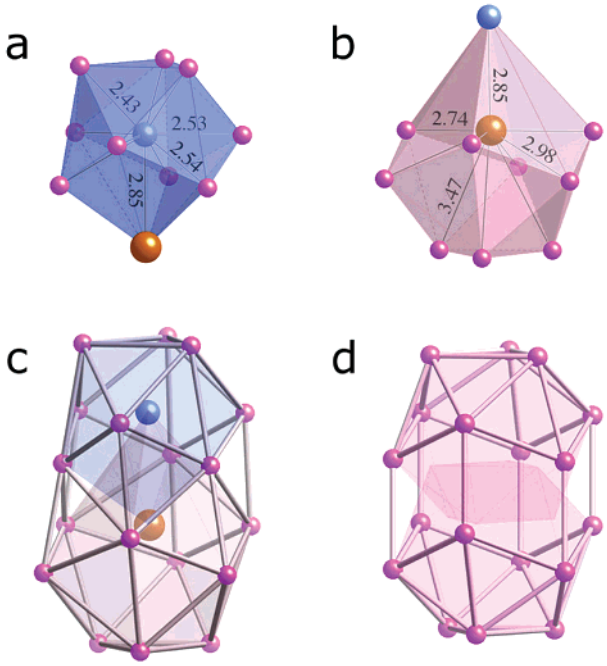

Figure 2. Polyhedral views of (a) [Mn@Al_9Ge] and (b) [Ge@Al_9Mn] clusters (Mn, blue; Ge, brown; Al, pink). (c) [MnGe@Al_{18}] cluster formed by interpenetration of the [Mn@Al_9Ge] and [Ge@Al_9Mn] clusters. (d) Al_{18} cluster modeled on the basis of Andersson's conjecture (see text). The cluster is formed by two icosahedra interpenetrating along a 3-fold axis.

with one Ge atom [Ge(2) in Table 2].[31] In Figure 1, it is noted that those [Mn@Al_9Ge] clusters (blue) are arranged in such a way that there are two sets of the clusters, each set forming a hexagonal lattice, and that the two sets are equivalent by inversion symmetry. Furthermore, the [Mn@Al_9Ge] clusters are surrounded by a larger "second" shell, and only the half portion of the shell structure is shown as a "half-broken" polyhedron in pale pink (see below). One unit cell contains two such shell structures, and the three-dimensional packing of the shell structures creates cube-shaped voids (green in Figure 1) centered on the unit cell edges along the *c*-axis, each of which is occupied by one Ge atom [Ge(1) in Table 2].

(29) Savrasov, S. Y. *LmtART 6.20*; Max-Planck-Institut für Festkorperforschung: Stuttgart, Germany, 2000.
(30) Vosko, S. H.; Wilk, L.; Nussair, M. *Can. J. Phys.* **1980**, *58*, 1200.
(31) A similar polyhedral structure (V@Ga_{10}) has been noted in the structure of V_8Ga_{41}. The same building unit exists in isostructural Zn-substituted compounds such as $V_8Ga_{36.9}Zn_{4.1}$, $Cr_8Ga_{29.8}Zn_{11.2}$, and $Mn_8Ga_{27.4}Zn_{13.6}$. See, for example, (a) Häussermann, U.; Viklund, P.; Svensson, C.; Eriksson, S.; Berastegui, P.; Lidin, S. *Angew. Chem., Int. Ed.* **1999**, *38*, 488, (b) Viklund, P.; Svensson, C.; Hull, S.; Simak, S. I.; Berastegui, P.; Häussermann, U. *Chem. Eur. J.* **2001**, *7*, 5143.

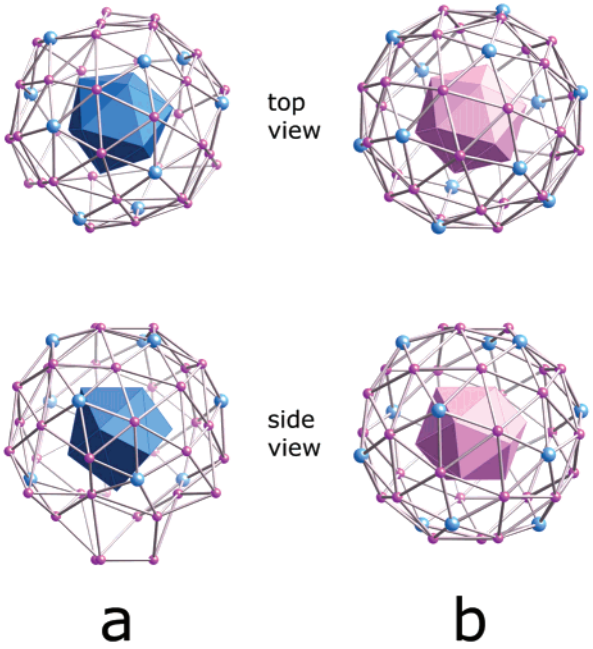

Figure 3. (a) Ball-and-stick view of the shell structure around the [Mn@Al_9Ge] cluster (blue polyhedron). The top and side views are along ⟨001⟩ and ⟨110⟩, respectively. Blue and pink atoms represent Mn and Al, respectively. In panel b, a Mackay icosahedron in α-MnAl(Si) is oriented along the corresponding directions. Mn atoms are shown as blue spheres, and Al and Si are mixed in the positions depicted as pink spheres.

Figure 2b depicts the polyhedral structure centered at a Ge(2) atom, that is, the Ge atom bonded to Mn atom in the [Mn@Al_9Ge] clusters (Figure 2a). While the symmetrical and topological nature of the cluster, formulated as [Ge@Al_9Mn], is identical to that of the [Mn@Al_9Ge] cluster, the actual shape of the former cluster is far from an icosahedron because of the widely scattered Ge−Al interatomic distances (2.74−3.47 Å) (Figure 2b). In the $Mn_{14}Al_{56+x}Ge_{3-x}$ structure, each [Ge@Al_9Mn] cluster conjoins one [Mn@Al_9Ge] cluster along the 3-fold axis parallel to the c-axis to form an elongated [MnGe@Al_{18}] cluster with the Mn and Ge atoms contained in an 18-vertex shell structure (Figure 2c). Because of the larger atomic size of Ge, the [MnGe@Al_{18}] cluster has a shape of a pear with longer atomic distances between the neighboring Ge and Al (d_{avg} = 2.98 Å) than between the Mn and Al (d_{avg} = 2.50 Å). Interestingly, a similar 18-membered shell structure, yet more symmetric, has been suggested by Andersson et al.[32] as a building block of quasicrystals, derived from the interpenetration of two icosahedra along a 3-fold axis (Figure 2d). However, such interpenetration may not be possible without a severe modification of the original icosahedra, as exemplified by the [MnGe@Al_{18}] in Figure 2c. This contrasts with the more familiar cluster formed by interpenetration of two icosahedra along a 5-fold axis in which the polyhedra maintain their shape by sharing five atoms.[5,33]

The most remarkable feature in the $Mn_{14}Al_{56+x}Ge_{3-x}$ structure is noted in the second shell structure that surrounds the [Mn@Al_9Ge] clusters (Figure 3a). The top half of the polyhedron manifests a dome structure made of all triangular faces,

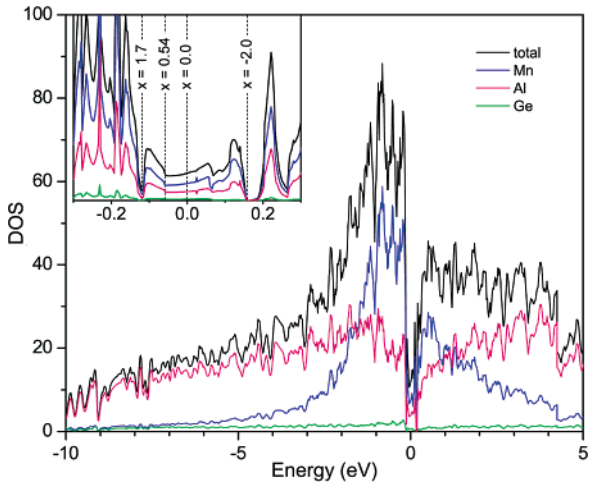

Figure 4. DOSs (states/eV cell) for the $Mn_{14}Al_{56}Ge_3$ compound from TB-LMTO-ASA calculations (total DOS, black; Mn contribution, blue; Al, red; Ge, green). The Fermi energy (E_F) = 0 eV. The pseudogap region near the E_F is zoomed in the inset. The vertical dashed lines indicate the Fermi levels for the corresponding x values in the formula $Mn_{14}Al_{56+x}Ge_{3-x}$, within a rigid band approximation.

while the ill-shaped bottom half is formed with randomly fused triangular and quadrangular faces. The apparently crushed shape of the bottom part is caused by the close-contact requirement for the Ge atom in [Mn@Al_9Ge] with the surrounding Al atoms. The triangular faces of the dome structure share their edges and corners to form pentagons and hexagons, and indeed the structure corresponds to half of a Mackay icosahedron (Figure 3b) in the α-MnAl(Si) structure.[34] The second shell of these "half-broken" Mackay icosahedra corresponds to the pale pink structures in Figure 1. It is striking to observe how persistently nature seeks to maintain (even a portion of) the high-symmetry polyhedral structure in this Mn−Al system. It is suspected that the existence of the Mackay icosahedra, although half-broken, in $Mn_{14}Al_{56+x}Ge_{3-x}$ may play an important role in structure stabilization.

Electronic Structure. To examine the electronic structure of the new phase, tight-binding linear muffin-tin orbital atomic sphere approximation (TB-LMTO-ASA) calculations were performed on the stoichiometric $Mn_{14}Al_{56}Ge_3$ as a representative model for the title phase. As shown in Figure 4, the calculated total DOS reveals a pseudogap at the Fermi energy with a width of ∼0.3 eV, indicative of weakly conducting behavior. The pseudogap is much narrower than the ones found in other aluminides whose complicated structures do not contain high-symmetry polyhedra.[14] Furthermore, the DOS values in Figure 4 change much more drastically right below and above the pseudogap, compared to those other aluminides.[14] The calculated DOS value at the Fermi energy, DOS(E_F), is ∼11 states/eV cell in Figure 4, and this value is much smaller than ∼24 states/eV cell[35] calculated for V_8Ga_{41}, whose structure contains V@Ga_{10} polyhedra similar to Mn@Al_9Ge but does not exhibit any larger high-symmetry second shell structure around V@Ga_{10}.[31] Indeed, these notable features in the DOS of the $Mn_{14}Al_{56}Ge_3$ are very similar to the findings in the electronic structure of $Mn_{12}Al_{57}$, an idealized stoichiometric model of the approximant α-Mn−

(32) Andersson, S.; Lidin, S.; Jacob, M.; Terasaki, O. *Angew. Chem., Int. Ed. Engl.* **1991**, *30*, 754.
(33) See, for example, Kreiner, G.; Franzen, H. F. *J. Alloys Compd.* **1995**, *221*, 15.
(34) (a) Robinson, K. *Acta Crystallogr.* **1952**, *5*, 397. (b) Cooper, M.; Robinson, K. *Acta Crystallogr.* **1966**, *20*, 614. (c) Sugiyama, K.; Kaji, N.; Hiraga, K. *Acta Crystallogr. C* **1998**, *54*, 445.
(35) The DOS(E_F) value was obtained from ref 31 after scaling with the number ratio of the atoms in the primitive cells of the two structures.

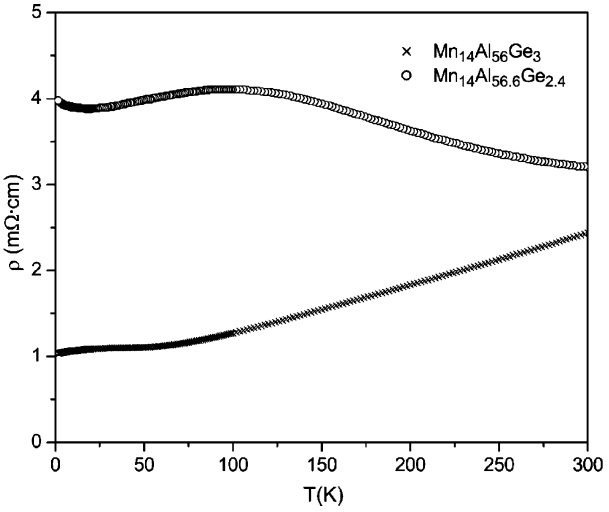

Figure 5. Temperature-dependent electrical resistivities of $Mn_{14}Al_{56}Ge_3$ (×) and $Mn_{14}Al_{56.6}Ge_{2.4}$ (○) from 1.8 to 300 K. The former is metallic, and the latter is semiconducting in the high-temperature region.

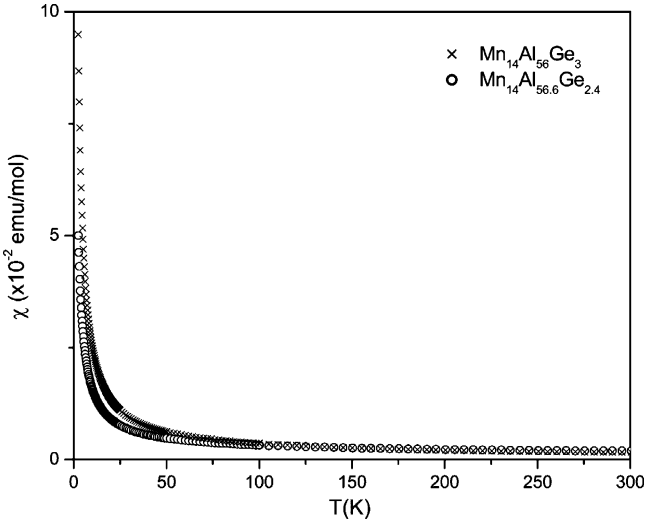

Figure 6. Temperature-dependent magnetic susceptibilities of $Mn_{14}Al_{56}Ge_3$ (×) and $Mn_{14}Al_{56.6}Ge_{2.4}$ (○) from 3 to 300 K, after diamagnetism correction.

Al−Si.[36] As in the case of α-Mn−Al−Si, the overall structural stabilization of $Mn_{14}Al_{56}Ge_3$ implies strong *covalent* interactions among the constituent atoms. The projected DOSs of Mn, Al, and Ge in Figure 4 conform to this argument in that they are well spread out in the pseudogap energy region in which Mn has a major contribution.

The calculated DOS in Figure 4 further provides insight into the question of the nonstoichiometries and partial substitution observed in our $Mn_{14}Al_{56+x}Ge_{3-x}$ phase. Within a rigid band approximation, the VEC, and hence the Fermi energy (E_F), decreases as x increases from zero, i.e., as the Ge sites become partially substituted by Al atoms. As clearly seen in the inset of Figure 4, this results in a gradual decrease in the total DOS to a minimum at the energy of −0.054 eV, which corresponds to $x = 0.54$ (indicated by a vertical dashed line). This compares well with $x = 0.61(2)$ (the corresponding $E_F = -0.059$ eV), the highest partial occupancy observed crystallographically among our samples. A similar explanation has already been suggested regarding the nonstoichiometry of α-Mn−Al−Si. The partial substitution of Al sites by Si atoms increases the Fermi energy to the point where the total DOS diminishes, and hence exploits, the structural stabilization with an optimum VEC.[37,38] Such energy points with zero DOS values exist also in the total DOS curve of the $Mn_{14}Al_{56}Ge_3$ above and below the E_F, as shown in the inset of Figure 4. With the corresponding x values of −2.0 and 1.7 (67% increase and 57% decrease in Ge content, respectively), however, we suspect that such a degree of atomic substitutions may not maintain the $Mn_{14}Al_{56+x}Ge_{3-x}$ structure because of the more drastic size difference between Ge and Al atoms than between Si and Al.

Physical Properties. In Figure 5, the measured specific resistivities of both $Mn_{14}Al_{56}Ge_3$ and $Mn_{14}Al_{56.6}Ge_{2.4}$ are high, in good agreement with the low DOS values at the E_F from the calculations, but they behave very differently from each other as the temperature changes, especially above 100 K; the first is metallic and the second is semiconducting. The complicated composition and temperature dependences of the resistivities are not unusual on account of their structural and electronic similarities to quasicrystals and the approximants for which various anomalous phenomena have been observed, including metal−insulator transitions, superconductivity, quantum-interference effects, and the Kondo effect.[2,6,13,37,38] The lower resistivity of the $Mn_{14}Al_{56}Ge_3$ is not caused by metallic impurities, such as aluminum metal that has been found in quenched samples in previous aluminide studies,[39] but is intrinsic to the sample. It is because such impurities are more likely in the Al-richer $Mn_{14}Al_{56.6}Ge_{2.4}$, which, however, behaves in the opposite way with a higher resistivity. The higher resistivity and metal−semiconductor transition of $Mn_{14}Al_{56.6}Ge_{2.4}$ could be from the enhanced scattering of the electrons by the partial occupancy in the structure.[40] Below 100 K, the scattering of electrons by the impurities is plausible for the cause of the resistivity minima (∼30 and ∼25 K for $Mn_{14}Al_{56}Ge_3$ and $Mn_{14}Al_{56.6}Ge_{2.4}$, respectively). In Figure 6, the measured magnetic susceptibilities of the two samples show Pauli paramagnetic behavior with a small amount of Curie components (2.4 and 1.5 at. % Mn, respectively, when $S = {}^5/_2$ is assumed). Although this could be caused by the magnetic impurities, it is not ruled out that a fraction of Mn atoms in the $Mn_{14}Al_{56+x}Ge_{3-x}$ phase may possess localized magnetic moments intrinsically.[41] The existence of nonzero magnetic moments is not unprecedented among the transition-metal quasicrystalline phases that show a pseudogap at the Fermi energy,[42] while the origin of the magnetism is still being debated.[43] The deformation of the local geometry around Mn atoms by the Ge atoms in the $Mn_{14}Al_{56+x}Ge_{3-x}$ structure

(36) Fujiwara, T. *Phys. Rev. B* **1989**, *40*, 942.
(37) Poon, S. J. *Adv. Phys.* **1992**, *41*, 303 and references therein.
(38) Zbigniew, M. S., Ed. *Physical Properties of Quasicrystals*; Springer: New York, 1999.
(39) (a) Klein, T.; Gozlan, A.; Berger, C.; Cyrot-Lackmann, F.; Calvayrac, Y.; Quivy, A. *Europhys. Lett.* **1990**, *13*, 129, (b) Mitutani, U.; Sakabe, Y.; Shibuya, T.; Kishi, K.; Kimura, K.; Takeuchi, S. *J. Phys. Condens. Matter* **1990**, *2*, 6169.
(40) (a) Anderson, P. W. *Phys. Rev.* **1958**, *109*, 1492. (b) Kamimura, H.; Aoki, H. *The Physics of Interacting Electrons in Disordered Systems*; Clarendon Press: Oxford, U.K., 1989. (c) Lee, K. S.; Seo, D.-K.; Whangbo, M.-H. *J. Solid State Chem.* **1997**, *134*, 5.
(41) For the magnetic properties of Mn−Al−Ge quasicrystals and approximants, see, for example, (a) Stadnik, Z. M.; Stroink, G. *Phys. Rev. B* **1991**, *43*, 894. (b) Hundley, M. F.; McHenry, M. E.; Dunlap, R. A.; Srinivas, V.; Bahadur, D. *Philos. Mag. B* **1992**, *66*, 239. (c) Lalla, N. P.; Tiwari, R. S.; Srivastava, O. N. *J. Mater. Res.* **1992**, *7*, 53.
(42) See, for example, (a) Bellissent, R.; Hippert, F.; Monod, P.; Vigneron, F. *Phys. Rev. B* **1987**, *36*, 5540. (b) Krajci, M.; Hafner, J. *Phys. Rev. B* **1998**, *58*, 14110. (c) Gomilsek, J. P.; Arcon, I.; Kodre, A.; Dolinsek, J. *Solid State Commun.* **2002**, *123*, 527.

could be a possible cause for the small Curie component found in our data.

Concluding Remarks

Despite their atomic ratios close to the Mn−Al−Si quasicrystalline phase and the approximants, the $Mn_{14}Al_{56+x}Ge_{3-x}$ phase, the Ge analogue, exhibits a structure that is an interesting variant that contains Mackay icosahedra that are half-broken. This is a remarkable example in which electronic tuning among the complicated network structures is realized both by the optimization of the electronic structure and by the introduction of nonstoichiometry, in response to structural perturbations caused by atomic size differences. More such compounds are expected to come when we introduce the size factor to such intermetallics, with possible changes in properties, as demonstrated in this work. We also believe that our new phase can serve as another model system for the future studies of structure−property relationships of quasicrystals and related compounds.

Acknowledgment. D.-K.S. is grateful to National Science Foundation for the financial support of this work through his NSF Career Award (DMR Contract 0239837). We thank Professor J. D. Corbett for helpful comments and Drs. S. L. Bud′ko and L. Chen for physical property measurements.

Supporting Information Available: Tables of selected single-crystal X-ray crystallographic data and CIF files of $Mn_{14}Al_{56+x}Ge_{3-x}$ ($x = 0$, 0.3, and 0.6). These materials are available free of charge via the Internet at http://pubs.acs.org.

JA039154F

(43) See, for example, (a) Dolinsek, J.; Klanjsek, M.; Apih, T.; Smontara, A.; Lasaunia, J. C.; Dubois, J. M.; Poon, S. J. *Phys. Rev. B* **2000**, *62*, 8862. (b) De Laissardiere, G. T.; Mayou, D. *Phys. Rev. Lett*. **2000**, *85*, 3273. (c) Dolinsek, J.; Klanjsek, M.; Apih, T.; Gailano, J. L.; Gianno, K.; Ott, H. R.; Dubois, J. M.; Urban, K. *Phys. Rev. B*. **2001**, *64*, 024203.